Analysis of Composite Plates Subjected to Impact Loading (Part II: Numerical Solution)[*]

Asst. Prof. Dr. Muhsin J. Jweeg
Mechanical Engineering Dept., College of Eng.
Al-Nahrain University, Baghdad, Iraq

Dr. Samera K. Radi
Mechanical Engineering Dept., College of Eng.
Al-Mustansiriya University, Baghdad, Iraq

Abstract

The search for a material, which is to be, light and at the same time strong, has resulted in the use of high strength, high modulus fibers reinforced in low strength, low modulus and low density matrix material which is called composite material.

The finite element models and numerical result are presented for impact of composite plates using a Special Third Order Theory (HOST 7) with the parabolic distribution of the transverse shear strain through the thickness of the plate and rotary inertia effect are taken into account.

The Newmark direct integration method is considered for the solution of linear dynamic response of the system. A typical finite element mesh of the quarter model is considered because of the double symmetric. A nine-noded Lagrangian element is chosen as a discretization element with seven degrees of freedom per node.

The effect of the velocity and mass of the impactor, number of layers, degree of orthotropy (E1/E2), lamination angle (θ)***, aspect ratio (a/b) and the boundary conditions on the dynamic response of the laminated plate is considered.***

The results show that the orthotropic ratio, velocity and mass of impactor have a significant effect on the deflection of the plate under impact load. In addition, the calculation of the dynamic load factor is presented.

الخلاصـــــة

البحث عن مواد خفيفة الوزن وقوية المتانة في نفس الوقت ادى الى استخدام الياف عالية المتانة في وسط ضعيف المتانة نسبيا" وهو مايدعى بالمواد المركبة. أستخدمت في هذا البحث طريقتي العناصر المحددة **(Finite Element)** *والحل الرقمي لتحليل تأثير احمال الصدم على المواد المركبة.*

النظرية الخامسة من الدرجة الثالثة **(HOST7)** *تم أستخدامها مع توزيع اجهادات القص خلال السمك على شكل قطع مكافىء، كذلك تم اختبار تأثير كتلة الواح المواد المركبة كما تم اخذ تأثير القصور الدوراني.*

الاستجابة الديناميكية الخطية تم تحليلها بأستخدام تكامل **(Newmark)** *المباشر. أستخدمت اجزاء محددة رباعية الطور بسبب التناظر المزدوج للاجزاء مع عنصر* **(Lagrangian)** *من تسع عقد وبسبع درجات حرية لكل عقدة.*

تم دراسة تأثير السرعة والكتلة للجسم الصادم مع عدد الطبقات ودرجة التعامدية **(E1/E2)** *وزاوية ميلان الالياف ونسبة ابعاد الالواح بالاضافة الى طريقة تثبيت الالواح.*

أظهرت النتائج ان درجة التعامدية **(E1/E2)** *والسرعة وكتلة الجسم الصادم لها تأثير ملحوظ على أنحناء الالواح المعرضة للصدم ،كذلك تم حساب معامل الحمل الديناميكي.*

[*] Republished Paper (Accepted for Publishing in 2002)

1. Introduction

Finite element procedures are very widely used in engineering analysis, and their applications are expected to increase significantly in the coming years. These procedures are employed extensively in the analysis of solids structures, heat transfer and fluids. Moreover, finite element methods are becoming more and more useful in virtually every field of engineering analysis.

The standard formulation for the finite element solution of solids is the displacement-based finite element method, which is widely used in the solution of practical problems. Practically, all major general-purpose analysis programs have been written using this formulation, because of its simplicity, generality and good numerical properties.

This work presents a special third order theory (HOST 7) for the dynamic analysis of unsymmetrically laminated multi-layered plates. A nine-nodded Lagrangian element is chosen as a discretization element with seven degrees-of-freedom per node.

C.T. Sun and S. Chattopadhyey [1] investigated the central impact of a mass on a simply supported-laminated composite plate under initial stress. B. V. Sanhar and C. T. Sun [2] used Finite element procedures to compute the impact response of graphite-epoxy laminated beam subjected to tensile initial stresses. H. Aggour and C. T. Sun [3] used in their study, a two dimensional finite element analysis for a fiber-reinforced composite laminate subjected to circularly distributed impact load. C. T. Sun and W. J. Liou [4] analyzed a laminated composite plate subjected to central small area impact loading. The Hertzian impact law was modelled to describe the contact force between the projectile and the laminated plate.

A. Nosier et. al. [5] studied the low velocity impact response of laminated plates by using a layer-wise theory. Six different modals were introduced for the representation of the impact pressure distribution. I. Smojver and I. Alfirevid [6] studied the problem of impact on layered composite and found that the behavior of composite laminates under impact loading depends not only upon the velocity but also on the mass and geometry of the impactor.

2. Theory Development of Impact

For the most general case the target is assumed to be a multilayer, generally orthotropic solid, whereas, the impactor is assumed to be a body of revolution. Moreover it is assumed that (1) the target and the impactor are linear elastic, (2) impact duration is long compared to stress-wave transit time in the impactor, (3) the impact is normal to the target surface, and (4) the area of contact is very small.

The rate of change of velocity during impact (as the two bodies come in contact) is:

$$m_1 \frac{dV_1}{dt} = -p \quad \text{..... (1)}$$

If we denote by the same distance that the impactor and target approach one another because of local compression at the point of contact, the velocity of this approach is:

$$\dot{\mu} = V_1 + V_2 \quad \text{..... (2)}$$

If the contact duration between the impactor and the target is very long in comparison with their natural periods, vibrations of the system can be neglected. Therefore, the Hertzian theory is applicable:

$$p = n_1 \mu^{3/2} \quad \text{..... (3)}$$

The term n_1 defined as:

$$n_1 = \frac{4\sqrt{R_1}}{2\pi(k_1 + k_2)} \quad \text{..... (4)}$$

where:

k1, k2: depend on the elastic constants of impactor and target and defined in [7]:

Differentiating (2), combining it with (1), and substituting (3) into the resulting equation yields:

$$\ddot{\mu} = \frac{-n_1}{m_1} \mu^{3/2} \quad \text{..... (5)}$$

If both sides of equ.(5) are multiplied by $\dot{\mu}$ and the resulting equation is integrated then we get:

$$\left(\dot{\mu}^2 - V^2\right) = -\frac{4}{5}\frac{n_1 \mu^{5/2}}{m_1} \quad \text{..... (6)}$$

where:

V: is the approach velocity of the two bodies at t=0, that is, at the beginning of impact.

Maximum deformation, μ_1, occurs when $\dot{\mu} = 0$ and is:

$$\mu_1 = \left(\frac{5 m_1 V^2}{4 n_1}\right)^{2/5} \quad \text{..... (7)}$$

Substituting of equ.(7) in to equ.(3) gives the following final relationship:

$$p = n_1^{2/5}\left(\frac{5m_1V^2}{4}\right)^{3/5} \quad \text{..... (8)}$$

For the case of the Hertzian contact problem involving a sphere pressed onto a flat surface by a force p, the area of contact is very small circle. Therefore, it may be assumed that the impact force is concentrated at that circle.

The maximum force p_o occurs at a time of $0.5t_o$ where t_o is the impact duration. The latter can be determined using an approach similar to that described by [8].

Solving equ.(6) for $\dot{\mu}$, yields:

$$\dot{\mu} = \left(V^2 - \frac{4}{5}\frac{n_1\mu^{5/2}}{m_1}\right)^{1/2} \quad \text{..... (9)}$$

Substituting $\dot{\mu} = d\mu / dt$ into equ. (9) and solving for dt:

$$dt = \frac{d\mu}{\left(V^2 - \frac{4n_1\mu^{5/2}}{5m_1}\right)^{1/2}} \quad \text{..... (10)}$$

Combining equ.(10) with equ.(7) and integrating to get:

$$t = \frac{2\mu_1}{V}\int_0^x \frac{dx}{\left(1 - x^{5/2}\right)^{1/2}} \quad \text{..... (11)}$$

where:

$x = (\mu / \mu_1)$.

The total impact duration, t_o, is obtained by the integration between the limits x=0 and x=1:

$$t_o = 2.94\frac{\mu_1}{V} = 2.94\left(\frac{5m_1}{4n_1V^{1/2}}\right)^{2/5} \quad \text{..... (12)}$$

The variation of impact force P with time can be determined numerically by integrating equ.(11) and expressing μ / μ_1 as a function of time t/t_o. The resulting curve can be approximated fairly accurately by the equation:

$$\mu = \mu_1 \sin\frac{\pi t}{t_o} \quad \text{..... (13)}$$

Substituting equ.(12) for t_o, to give:

$$\mu = \mu_1 \sin\frac{\pi\, t\, V}{2.94\mu_1} \quad \text{..... (14)}$$

Combining equs.(14) and (3) yields the following expressions for p as a function of time, t:

$$p(t) = p_o\left[\sin\frac{\pi t V}{2.94\mu_1}\right]^{3/2} \quad \text{..... (15)}$$

where:

$$p_o = n_1^{2/5}\left[\frac{5m_1V^2}{4}\right]^{3/5}$$

3. Special Third-Order Theory (HOST 7)

The special third-order theory, which presents displacement components, is given in the form [9]:

$$\begin{aligned} u(x,y,z,t) &= u_o(x,y,t) + z\phi_x(x,y,t) + z^3\theta_x(x,y,t) \\ v(x,y,z,t) &= v_o(x,y,t) + z\phi_y(x,y,t) + z^3\theta_y(x,y,t) \\ w(x,y,z,t) &= w_o(x,y,t) \end{aligned} \quad \text{..... (16)}$$

where:

(u_o, v_o, w_o): denote the displacement of a point on the mid-surface of the plate(z=0),

ϕ_x and ϕ_y: are the rotations of the transverse normal in the xz and yz planes.

The term θ_x, θ_y can be interpreted as the stretching of the transverse normal, for the remaining higher-order term.

The strain-displacement relations, using the above displacement forms, may be written as:

$$\varepsilon_x = \frac{\partial u}{\partial x} = \frac{\partial u_o}{\partial x} + z\frac{\partial \phi_x}{\partial x} + z^3\frac{\partial \theta_x}{\partial x}$$

$$\varepsilon_y = \frac{\partial v}{\partial y} = \frac{\partial v_o}{\partial y} + z\frac{\partial \phi_y}{\partial y} + z^3\frac{\partial \theta_y}{\partial y}$$

$$\varepsilon_z = \frac{\partial w}{\partial z} = 0$$

$$\gamma_{xy} = \frac{\partial u}{\partial y} + \frac{\partial v}{\partial x} = \left(\frac{\partial u_o}{\partial y} + \frac{\partial v_o}{\partial x}\right) + z\left(\frac{\partial \phi_x}{\partial y} + \frac{\partial \phi_y}{\partial x}\right) + z^3\left(\frac{\partial \theta_x}{\partial y} + \frac{\partial \theta_y}{\partial x}\right) \quad \text{..... (17)}$$

$$\gamma_{yz} = \frac{\partial v}{\partial z} + \frac{\partial w}{\partial y} = \phi_y + \frac{\partial w_o}{\partial y} + z^2\left(3\theta_y\right)$$

$$\gamma_{xz} = \frac{\partial u}{\partial z} + \frac{\partial w}{\partial x} = \phi_x + \frac{\partial w_o}{\partial x} + z^2\left(3\theta_x\right)$$

or:

$$\begin{Bmatrix}\varepsilon_x\\ \varepsilon_y\\ \gamma_{xy}\end{Bmatrix} = \begin{Bmatrix}\varepsilon_x^o\\ \varepsilon_y^o\\ \gamma_{xy}^o\end{Bmatrix} + z\begin{Bmatrix}R_x\\ R_y\\ R_{xy}\end{Bmatrix} + z^3\begin{Bmatrix}S_x\\ S_y\\ S_{xy}\end{Bmatrix} \qquad \begin{Bmatrix}\gamma_{yz}\\ \gamma_{xz}\end{Bmatrix} = \begin{Bmatrix}\phi_y + \frac{\partial w_o}{\partial y}\\ \phi_x + \frac{\partial w_o}{\partial x}\end{Bmatrix} + 3z^2\begin{Bmatrix}\theta_y\\ \theta_x\end{Bmatrix} \quad \text{..... (18)}$$

where,

$$\begin{Bmatrix}\varepsilon_x^o\\ \varepsilon_y^o\\ \gamma_{xy}^o\end{Bmatrix} = \begin{Bmatrix}\frac{\partial u_o}{\partial x}\\ \frac{\partial v_o}{\partial y}\\ \frac{\partial u_o}{\partial y} + \frac{\partial v_o}{\partial x}\end{Bmatrix}, \begin{Bmatrix}R_x\\ R_y\\ R_{xy}\end{Bmatrix} = \begin{Bmatrix}\frac{\partial \phi_x}{\partial x}\\ \frac{\partial \phi_y}{\partial y}\\ \frac{\partial \phi_x}{\partial y} + \frac{\partial \phi_y}{\partial x}\end{Bmatrix}, \begin{Bmatrix}S_x\\ S_y\\ S_{xy}\end{Bmatrix} = \begin{Bmatrix}\frac{\partial \theta_x}{\partial x}\\ \frac{\partial \theta_y}{\partial y}\\ \frac{\partial \theta_x}{\partial y} + \frac{\partial \theta_y}{\partial x}\end{Bmatrix} \quad \text{..... (18)}$$

Substituting equs.(18) in the stress-strain relation of the lamina, the constitutive relations for any layer in the (x, y) system are in the form [7]:

$$\begin{Bmatrix}\sigma_x\\ \sigma_y\\ \tau_{xy}\end{Bmatrix}_k = \begin{bmatrix}\overline{Q}_{11} & \overline{Q}_{12} & \overline{Q}_{16}\\ \overline{Q}_{12} & \overline{Q}_{22} & \overline{Q}_{26}\\ \overline{Q}_{16} & \overline{Q}_{26} & \overline{Q}_{66}\end{bmatrix}_k \left\{\begin{Bmatrix}\varepsilon_x^o\\ \varepsilon_y^o\\ \gamma_{xy}^o\end{Bmatrix} + z\begin{Bmatrix}R_x\\ R_y\\ R_{xy}\end{Bmatrix} + z^3\begin{Bmatrix}S_x\\ S_y\\ S_{xy}\end{Bmatrix}\right\} \quad \text{..... (20 a)}$$

$$\begin{Bmatrix}\tau_{yz}\\ \tau_{xz}\end{Bmatrix}_k = \begin{bmatrix}\overline{Q}_{44} & \overline{Q}_{45}\\ \overline{Q}_{45} & \overline{Q}_{55}\end{bmatrix}_k \left\{\begin{Bmatrix}\phi_y + \frac{\partial w_o}{\partial y}\\ \phi_x + \frac{\partial w_o}{\partial x}\end{Bmatrix} + 3z^2\begin{Bmatrix}\theta_y\\ \theta_x\end{Bmatrix}\right\} \quad \text{..... (20 b)}$$

where:

$$[\bar{Q}]=[T]^T[Q][T] \quad \text{..... (21)}$$

[T]: Transformation matrix given by:

$$[T]=\begin{bmatrix} c^2 & s^2 & sc & 0 & 0 \\ s^2 & c^2 & -sc & 0 & 0 \\ -2sc & 2sc & c^2-s^2 & 0 & 0 \\ 0 & 0 & 0 & c & -s \\ 0 & 0 & 0 & s & c \end{bmatrix}$$

where:

c: cos θ, s =sin θ

$Q_{11}=E_1/(1-\nu_{12}\nu_{21})$, $Q_{12}=\nu_{12}E_1(1-\nu_{12}\nu_{21})$, $Q_{22}=E_2/(1-\nu_{12}\nu_{21})$,

$Q_{33}=G_{12}$, $Q_{44}=G_{23}$, $Q_{55}=G_{13}$

The transformation equ.(3.52) can be represented in the following form:

$$\begin{aligned}
\bar{Q}_{11}&=Q_{11}c^4+2(Q_{12}+2Q_{33})s^2c^2+Q_{22}s^4 \\
\bar{Q}_{12}&=(Q_{11}+Q_{22}-4Q_{33})s^2c^2+Q_{12}(s^4+c^4) \\
\bar{Q}_{22}&=Q_{11}s^4+2(Q_{12}+2Q_{33})s^2c^2+Q_{22}c^4 \\
\bar{Q}_{16}&=(Q_{11}-Q_{12}-2Q_{33})sc^3+(Q_{12}-Q_{22}+2Q_{33})s^3c \quad \text{..... (22)} \\
\bar{Q}_{26}&=(Q_{11}-Q_{12}-2Q_{33})cs^3+(Q_{12}-Q_{22}+2Q_{33})sc^3 \\
\bar{Q}_{66}&=(Q_{66}+Q_{22}-2Q_{12}-2Q_{33})s^2c^2+Q_{33}(s^4+c^4) \\
\bar{Q}_{44}&=Q_{44}c^2+Q_{55}s^2 \\
\bar{Q}_{45}&=(Q_{55}-Q_{44})sc \\
\bar{Q}_{55}&=Q_{44}s^2+Q_{55}c^2
\end{aligned}$$

All other elements of $[Q_{ij}]$ and $[\bar{Q}_{ij}]$ are zero.

4. Formulation of Elasticity Matrix of Composite Laminated Plates

In the following procedure, the elasticity matrix [D] is evaluated based on the special third order shear deformation theory [equs.(16)]. The following definition for stress-strain is resultant expressions appropriate to the special third order shear deformation theory:

$$\begin{bmatrix} N_x & M_x & M_x^* \\ N_y & M_y & M_y^* \\ N_{xy} & M_{xy} & M_{xy}^* \end{bmatrix} = \sum_{L=1}^{N} \int_{h_l}^{h_{L+1}} \begin{bmatrix} \sigma_x \\ \sigma_y \\ \sigma_{xy} \end{bmatrix} \left(1 \ , \ z \ , \ z^3\right) dz \quad \text{..... (23 a)}$$

$$\begin{bmatrix} Q_x & Q_x^* \\ Q_y & Q_y^* \end{bmatrix} = \sum_{L=1}^{N} \int_{h_l}^{h_{L+1}} \begin{bmatrix} \tau_{xz} \\ \tau_{yz} \end{bmatrix} \left(1 \ , \ z^2\right) dz \quad \text{..... (23 b)}$$

By substituting equs.(20) for stresses vectors in equs.(23) and integrating with respect to z, the stress-resultants are obtained in terms of the seven generalized displacements as [9]:

$$\{\bar{\sigma}\} = [D]\{\bar{\varepsilon}\} \quad \text{..... (24 a)}$$

$$\begin{bmatrix} N_x \\ N_y \\ N_{xy} \\ M_x \\ M_y \\ M_{xy} \\ M_x^{\bullet} \\ M_y^{\bullet} \\ M_{xy}^{\bullet} \end{bmatrix} = \sum_{L=1}^{n} \begin{bmatrix} \bar{Q}_{11}H_1 & \bar{Q}_{12}H_1 & \bar{Q}_{13}H_1 & \bar{Q}_{11}H_2 & \bar{Q}_{12}H_2 & \bar{Q}_{13}H_2 & \bar{Q}_{11}H_4 & \bar{Q}_{12}H_4 & \bar{Q}_{13}H_4 \\ & \bar{Q}_{22}H_1 & \bar{Q}_{23}H_1 & \bar{Q}_{12}H_2 & \bar{Q}_{22}H_2 & \bar{Q}_{23}H_2 & \bar{Q}_{12}H_4 & \bar{Q}_{22}H_4 & \bar{Q}_{23}H_4 \\ & & \bar{Q}_{33}H_1 & \bar{Q}_{13}H_2 & \bar{Q}_{23}H_2 & \bar{Q}_{33}H_2 & \bar{Q}_{13}H_4 & \bar{Q}_{23}H_4 & \bar{Q}_{33}H_4 \\ & & & \bar{Q}_{11}H_3 & \bar{Q}_{12}H_3 & \bar{Q}_{13}H_3 & \bar{Q}_{11}H_5 & \bar{Q}_{12}H_5 & \bar{Q}_{13}H_5 \\ & & & & \bar{Q}_{22}H_3 & \bar{Q}_{23}H_3 & \bar{Q}_{12}H_5 & \bar{Q}_{22}H_5 & \bar{Q}_{23}H_5 \\ & & & & & \bar{Q}_{33}H_3 & \bar{Q}_{13}H_5 & \bar{Q}_{23}H_5 & \bar{Q}_{33}H_5 \\ & & & & & & \bar{Q}_{11}H_7 & \bar{Q}_{12}H_7 & \bar{Q}_{13}H_7 \\ & & & & & & & \bar{Q}_{22}H_7 & \bar{Q}_{23}H_7 \\ & & & & & & & & \bar{Q}_{33}H_7 \end{bmatrix} \begin{bmatrix} \frac{\partial u_\circ}{\partial x} \\ \frac{\partial v_\circ}{\partial y} \\ \frac{\partial u_\circ}{\partial y} + \frac{\partial v_\circ}{\partial x} \\ \frac{\partial \phi_x}{\partial x} \\ \frac{\partial \phi_y}{\partial y} \\ \frac{\partial \phi_x}{\partial y} + \frac{\partial \phi_y}{\partial x} \\ \frac{\partial \theta_x}{\partial x} \\ \frac{\partial \theta_y}{\partial y} \\ \frac{\partial \theta_x}{\partial y} + \frac{\partial \theta_y}{\partial x} \end{bmatrix} \quad \text{... (24 b)}$$

$$\begin{bmatrix} Q_x \\ Q_y \\ Q_x^{\bullet} \\ Q_y^{\bullet} \end{bmatrix} = \sum_{L=1}^{N} \begin{bmatrix} \bar{Q}_{55}H_1 & \bar{Q}_{45}H_1 & \bar{Q}_{55}H_3 & \bar{Q}_{45}H_3 \\ & \bar{Q}_{44}H_1 & \bar{Q}_{45}H_3 & \bar{Q}_{44}H_3 \\ & & \bar{Q}_{55}H_5 & \bar{Q}_{45}H_5 \\ & \text{SYMMETRIC} & & \bar{Q}_{44}H_5 \end{bmatrix} \begin{bmatrix} \phi_x + \partial w_\circ / \partial x \\ \phi_y + \partial w_\circ / \partial y \\ 3\theta_x \\ 3\theta_y \end{bmatrix} \quad \text{..... (24 c)}$$

In the above relations, N is the number of layers and

$$H_i = \frac{1}{i}\left(h_{L+1}^i - h_L^i\right), \ i = 1, 2, 3, 4, 5, 7 \quad \text{..... (24 d)}$$

5. Element Stiffness Matrix

The element under consideration is a nine-node Lagrangian quadrilateral isoparametric element. At any point, the continuum displacement vector within the element is discretized such that:

$$\{\delta\} = \sum_{i=1}^{NN} N_i \{\delta_i\} \quad \text{..... (25)}$$

where:

Ni: is the shape function associated with node i,

NN: is the number of nodes in an element and:

$$\{\delta_i\} = \{u_{oi}, v_{oi}, w_{oi}, \phi_{xi}, \phi_{yi}, \theta_{xi}, \theta_{yi}\}^T \quad \text{..... (26)}$$

The generalized strain $\bar{\varepsilon}$ at any point within an element can be expressed by the following relationship:

$$\{\bar{\varepsilon}\} = \sum_{i=1}^{NN} B_i \{\delta i\} \quad \text{..... (27 a)}$$

where:

$$\bar{\varepsilon} = \left[\frac{\partial u_o}{\partial x}, \frac{\partial v_o}{\partial y}, \frac{\partial u_o}{\partial y} + \frac{\partial v_o}{\partial x}, \frac{\partial \phi_x}{\partial x}, \frac{\partial \phi_y}{\partial y}, \frac{\partial \phi_x}{\partial y} + \frac{\partial \phi_y}{\partial x}, \frac{\partial \theta_x}{\partial x}, \frac{\partial \theta_y}{\partial y}, \frac{\partial \theta_x}{\partial y} + \frac{\partial \theta_y}{\partial x}, \phi_x + \frac{\partial w_o}{\partial x}, \phi_y + \frac{\partial w_o}{\partial y}, 3\theta_x, 3\theta_y \right]^T \quad \text{..... (27 b)}$$

Elements of non-zero terms of strain-displacement matrix [B] are given as [9]:

$$\begin{aligned} &B_{1,1} = B_{3,2} = B_{4,4} = B_{6,5} = B_{7,6} = B_{9,7} = B_{10,3} = \frac{\partial N_i}{\partial x} \\ &B_{10,4} = B_{11,5} = N_i \\ &B_{2,2} = B_{3,1} = B_{5,5} = B_{6,4} = B_{8,7} = B_{9,6} = B_{11,3} = \frac{\partial N_i}{\partial y} \\ &B_{12,6} = B_{13,7} = 3N_i \end{aligned} \quad \text{..... (28)}$$

Upon evaluating the D and Bi matrices as given by equs.(24) and (28) respectively, the element stiffness matrix can be readily computed using the standard relation:

$$[K] = \int_A [B]^T [D][B] dA \quad \text{..... (29)}$$

6. Element Mass Matrix

A mass matrix of fiber-reinforced laminated plate is derived from a consistent matrix. It is called "Consistent" because the same displacement model, used for deriving the element stiffness matrix, is used for the derivation of mass matrix. The mass $[M]^e$ is given by [9],

$$[M]^e = \int_A [N]^T [m][N] dA \quad \text{..... (30)}$$

where:

$$[N]=[N_1, N_2 \ldots N_{NN}] \quad \text{..... (30 a)}$$

$$[m] = \begin{bmatrix} I_1 & & & & & & \\ & I_1 & & & & & \\ & & I_1 & & 0 & & \\ & & & I_2 & & & \\ & & 0 & & I_2 & & \\ & & & & & I_3 & \\ & & & & & & I_3 \end{bmatrix} \quad \text{..... (30 b)}$$

In which,

$$(I_1, I_2, I_3) = \sum_{L=1}^{n} \int_{h_L}^{h_{L+1}} (1, z^2, z^6) \rho^L dz \quad \text{..... (31)}$$

where:

ρ^L : is the material density of the L^{th} layer,

I_1, I_2 and I_3: are normal inertia, rotary inertia and higher-order inertia terms respectively.

7. Solution of Equilibrium Equations in Dynamic Analysis

The equations of equilibrium governing the linear dynamic response of a system of finite elements are derived:

$$M\ddot{U} + KU = R \quad \text{..... (32)}$$

where:

M and K: are the mass and stiffness matrices;

R: is the vector of externally applied loads;

U and $\ddot{U}$: are the displacement and acceleration vectors of the finite element assemblage.

It should be recalled that equ.(32) is derived from static considerations at time t; i.e., equ.(32) may be written as:

$$F_I(t) + F_E(t) = R(t) \quad \text{..... (33)}$$

where:

$F_I(t)$ are the inertia forces,

$F_I(t) = M\ddot{U}$

$F_E(t)$ are the elastic forces,

$F_E(t) = KU$

In this work the direct integration methods namely the Newmark method is considered for the solution of equ.(32).

8. Results and Discussion

In finite element discretization of laminated plates only one quarter of the plate was considered in most of the studied cases, due to double symmetry about x- and y- axes.

In the following it is assumed that the material is fiber- reinforced and remains in the elastic range.

The material properties are:

$E_2=6{,}62x10^9\ N/m^2$, $E_1=40E_2$, $G_{12}=G_{13}=0.5E_2$, $G_{23}=0.6E_2$, $\nu_{12}=0.25$

Dimensions of plate:

$a=1\ m$, $b=1\ m$, $h=0.02\ m$

Properties of impactor:

$E=200\ x\ 10^6\ N/m^2$, $\nu=0.3$, $mass=0.1\ kg$, $Radius=0.01\ m$

From **Figs.(1)** and **(2)**, it can be seen that the deflection predicted in the present study using HOST 7 agrees very well with the numerical solution [5] and experimental studying [10] respectively.

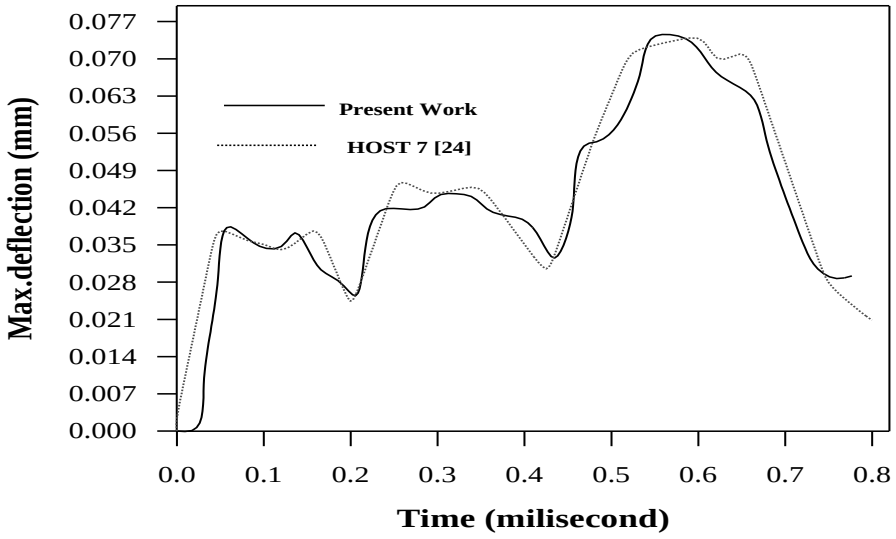

Figure (1) Comparison the present work with the numerical solution of [5] of simply supported plate

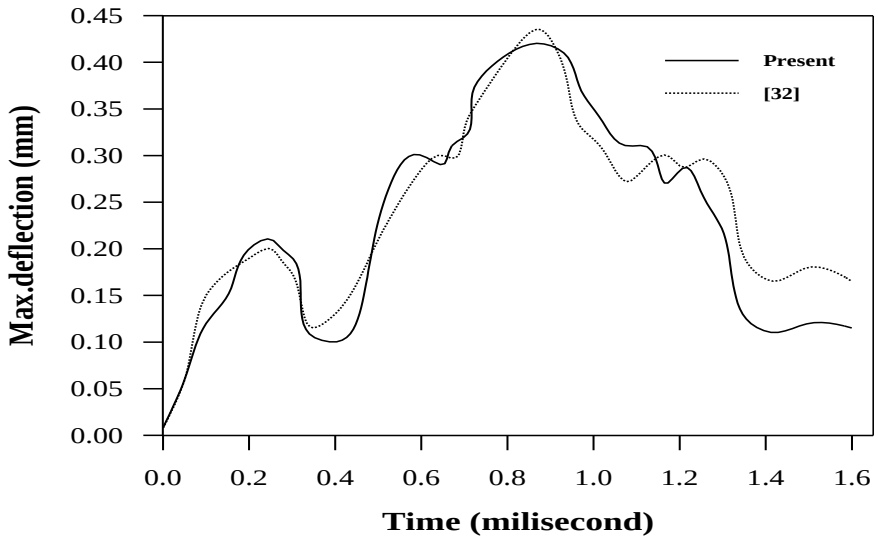

Figure (2) Comparison the present work with the experimental study of [10] of simply supported plate

Figure (3) shows the effect of velocity of impactor on the impact force history. It can be seen that as the velocity of impactor increases the impact force increases and the impact duration decreases.

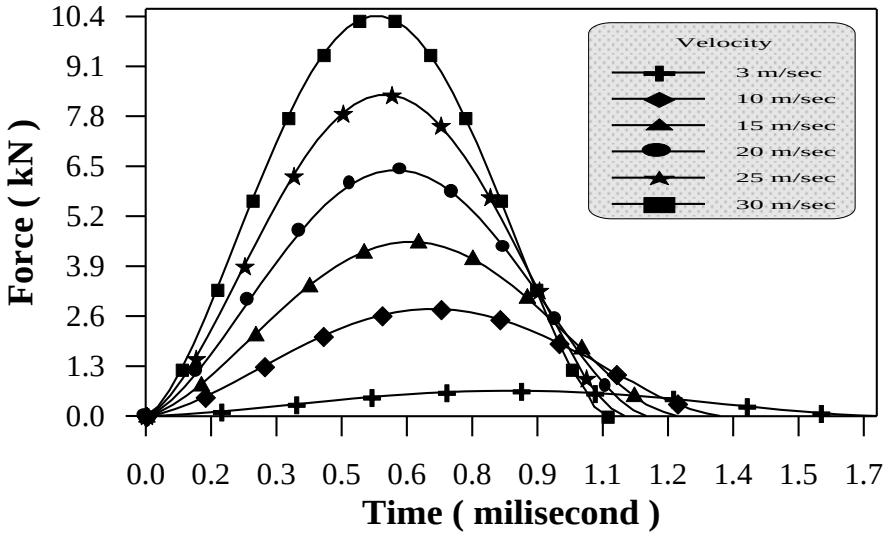

Figure (3) Effect of variation the velocity of impactor on the contact force histories (mass=0.1 kg)

Figure (4) shows the effect of mass of impactor on the impact force history. It is seen that both of the impact force and the duration increases with the increase of the impactor's mass.

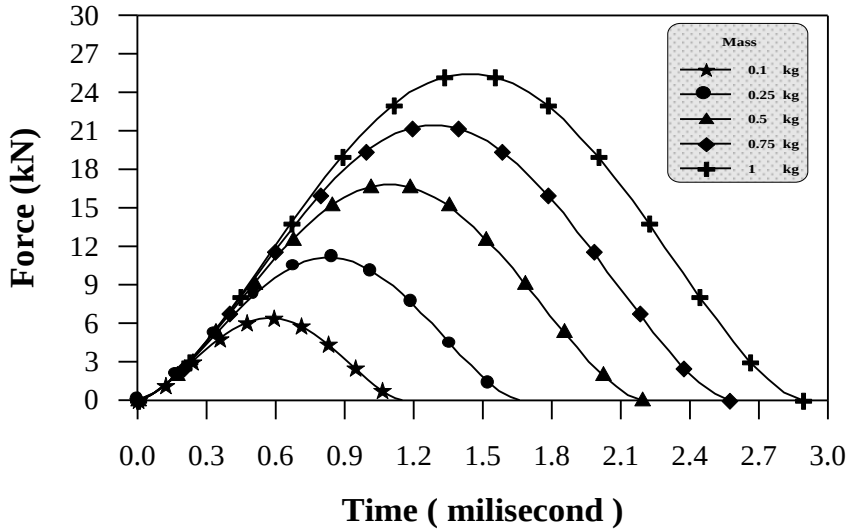

Figure (4) Effect of variation the mass of impactor on the contact force histories (V=20 m/sec)

Form **Figs.(3)** and **(4)** it can be seen that increasing mass or velocity of impactor results in an increase in the impact force due to the increase of energy absorbed from the plate. With the increase of impactor mass the duration of impact increases because of the high inertia of impactor.

From **Fig.(5)** it can be seen that the coupling has a noticeable influence on the response of the two-layer plate, while the coupling dies out as the number of layers increases. The central deflection decreases with the increase in the number of layers. This trend, again, is observed for antisymmetric cross-ply laminates in **Fig.(6)**.

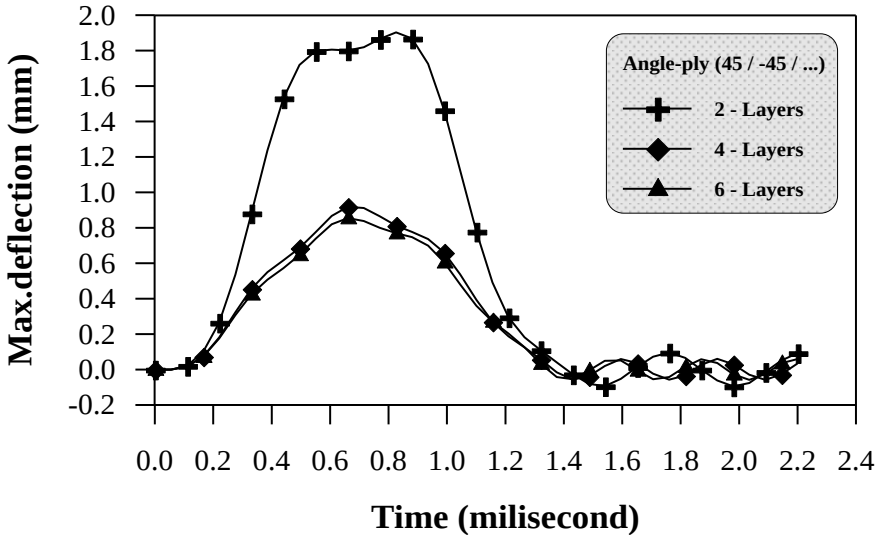

Figure (5) Effect of number of layers on a transient response of a square antisymmetric angle-ply laminated plate (V=10 m/sec)

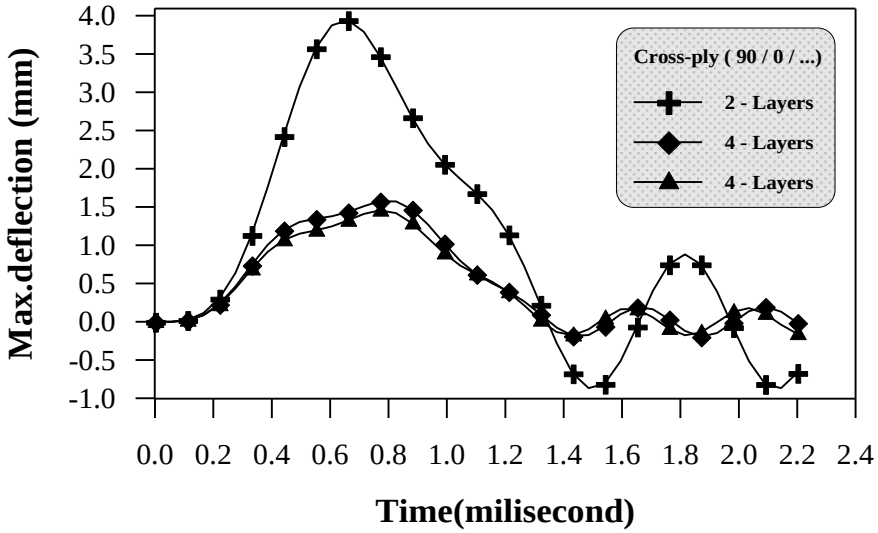

Figure (6) Effect of number of layers on a transient response of a square antisymmetric cross-ply laminated plate (V=10 m/sec)

Figure (7) presents the effect of the degree of orthotropy (E_1/E_2). It can be seen that an increase in the material orthotropy ratio (E1/E2) results in a decrease in the central deflection due to the increase in the plate stiffness.

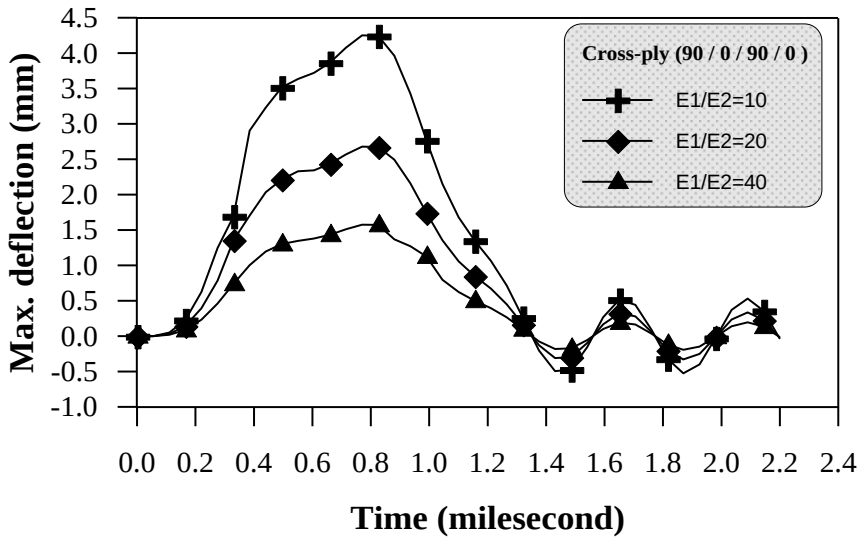

Figure (7) Effect of orthotropic ratio on a transient response of a square antisymmetric cross-ply laminated plate (V=10m/sec)

Figure (8) shows the effect of the lamination angle (θ^o) on the transient response of antisymmetric square plate. It is apparent from the results that the transverse deflection decreases with the increase in the angle of lamination from θ^o = 0 to 45 due to the increase in plate stiffness. The relation is symmetric about (θ^o = 45^o) i.e. central deflection reduces at the same rate when (θ^o) increases from 45^o to 90^o.

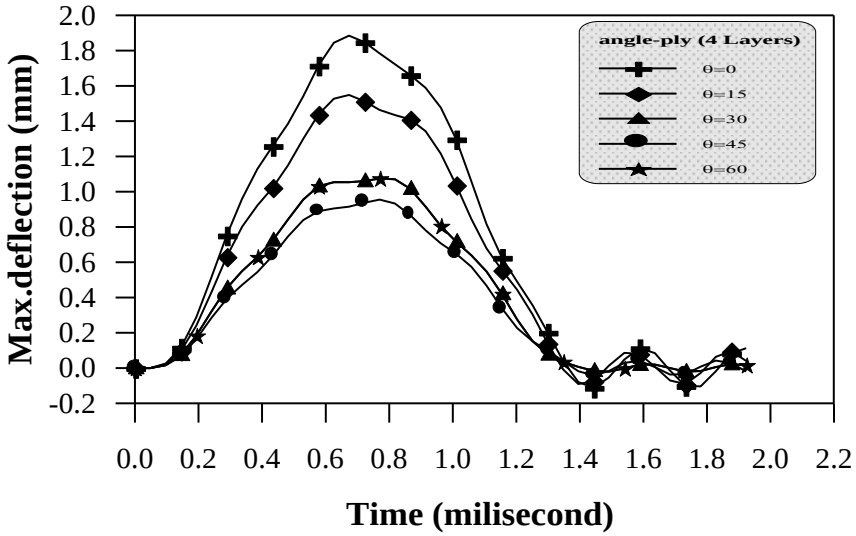

Figure (8) Effect of lamination angle on a transient response of a square antisymmetric angle-ply laminated plate $(\theta,-\theta,\theta,-\theta)$ (V=10 m/sec)

Figure (8) illustrates the effect of the aspect ratio (a/b) on the transient response of the antisymmetric cross-ply ($90^o/0^o/90^o/0^o$). It is clear that the aspect ratio (a/b) is noticeable, and the maximum deflection occurs when the plate is square, otherwise the deflection decreases.

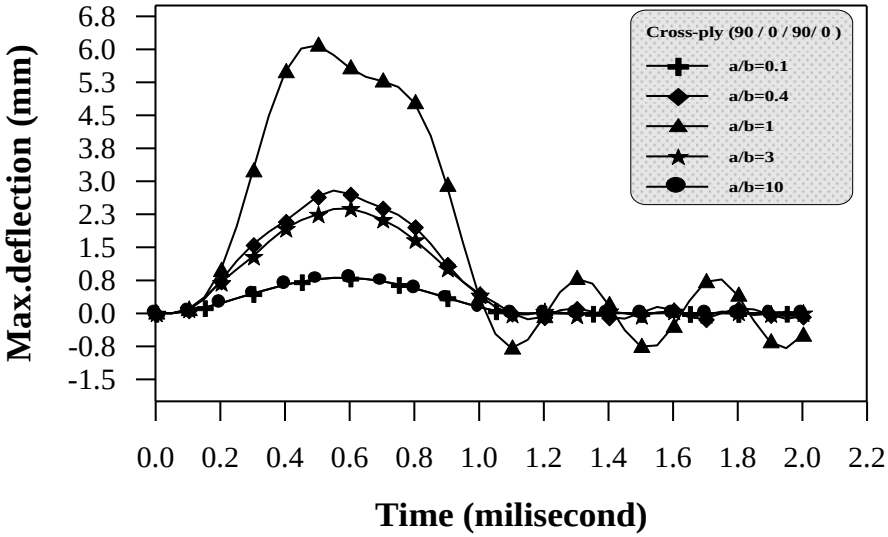

Figure (9) Effect of aspect ratio on a transient response of a square antisymmetric cross-ply laminated plate (area=1m^2) (V=30 m/sec)

Figure (10) indicates the effect of boundary conditions on the central deflection for antisymmetric cross-ply (90/0/90/0) laminated plate. As it is seen in this figure, the minimum deflection occurs when the plate is clamped along all edges due to the increase in the plate stiffness.

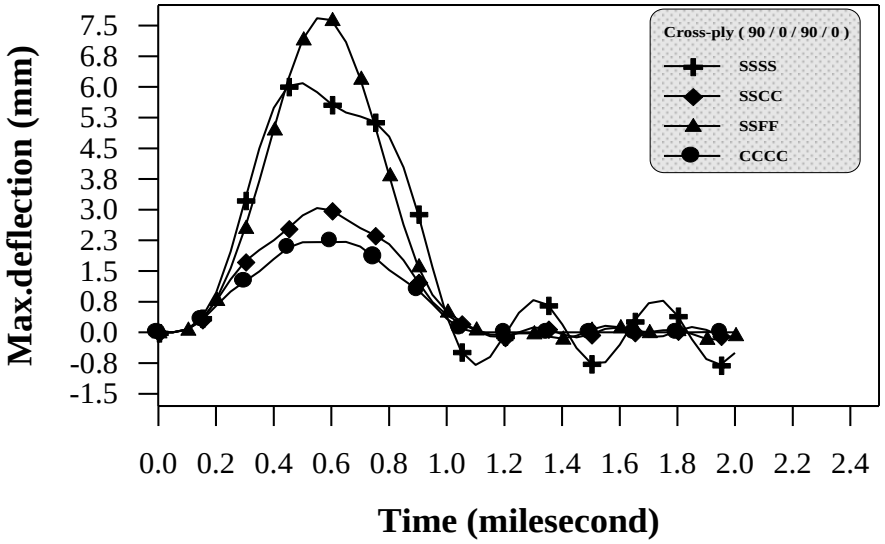

Figure (10) Effect of boundary conditions on a transient response of a square antisymmetric cross-ply laminated plate (V=30 m/sec)

Finally, from the dynamic analysis, the dynamic load factor (D.L.F) can be calculated from:

$$\text{D.L.F} = \frac{\text{Max .deflection in dynamic}}{\text{Max .deflection in static (Part I)}}$$

The range of (D.L.F) was between $(1.9 \rightarrow 2.2)$ which depending on the properties of target, mass, velocity and properties of impactor.

9. Conclusions

The main conclusions of this work for dynamic analyses of multilayer composite plates may be summarized as:

1. Increasing the velocity of impactor increases impact force and reduces impact duration.
2. Increasing mass of impactor increases impact force and duration.
3. The central deflection decreases with the increase in the number of layers.
4. An increase in orthotropy ratio (E_1/E_2) results in a decrease in the amplitude.
5. For an angle-ply laminated plate, it is found that, $(\theta = 45^o)$ represents the best lamination angle at which minimum deflection is achieved.
6. Maximum amplitude occurs when aspect ratio is equal to one.
7. The clamped boundary conditions for all plate edges give minimum deflection.
8. The range of dynamic load factor for composite plate under impact loading is between $(1.9 \rightarrow 2.2)$.

10. References

1. C. T., Sun, and S., Chattopadhyey, ***"Dynamic Response of Anisotropic Laminated Plates under Initial Stress to Impact of a Mass"***, Journal of Applied Mechanics, September 1975, pp. 693-698.

2. B. V., Sankar, and C. T., Sun, ***"Low-Velocity Impact Response of Laminated Beams Subjected to Initial Stresses"***, AIAA Journal, Vol. 23, 1985, pp. 1962-1969.

3. H., Aggour, and C. T., Sun, ***"Finite Element Analysis of a Laminated Composite Plate Subjected to Circularly Distributed Central Impact Loading"***, Computers and Structures, Vol. 28, No. 6, 1988, pp. 729-736.

4. C. T., Sun, and W. J., Lion, ***"Investigation of Laminated Composite Plates Under Impact Dynamic Loading Using a Three-Dimensional Hybrid Stress Finite Element Method"***, Computers and Structures, Vol. 33, No. 3, 1989, pp. 879-864.

5. A., Nosie, R. K., Kapania, and J. N., Reddy, ***"Low-Velocity Impact of Laminated Composites Using a Layer Wise Theory"***, Virginia Polytechnique Institute and State University, USA, 1994.

6. Smojver, and I., Alfirevic, ***"The Influence of Impact Damage on Design of Composite Structures"***, International Design Conference-Design 2000, May 23-26, 2000.

7. F. A., Abdulla, ***"Analysis of Composite Plate Subjected to Impact Load"***, M.Sc., Thesis, Al-Mustansiriya University, Mech. Eng. Dept., 2001.

8. A. Z., Jonas, ***"Impact Dynamic"***, by John Wily & Sons, Inc., 1982.

9. T., Kant, and Mallikarjuna, ***"A Higher-Order Theory for Free Vibration of Unsymmetrically Laminated Composite and Sandwich Plates-Finite Element Evaluations"***, Computers and Structures, Vol. 32, No. 5, 1989, pp. 1125-1132.

10. S. C., Douglas, and A. L., Paul, ***"Transient Response of Graphite/Epoxy and Kelvar/Epoxy Laminated Subjected to Impact"***, AIAA Journal, Vol. 27, No. 11, 1988, pp. 1590-1596.

List of Symbols

A	Area integral indicator.
E_1,E_2	Modulus of elasticity in 1 and 2 directions (N/m^2) respectively.
G_{12},G_{23},G_{13}	Modulus of rigidity in 1-2 ,2-3 and 1-3 planes (N/m^2) respectively.
H	Laminated thickness (m).
h_L,h_{L-1}	Distance from plate middle surface to the lower and upper surface of i^{th} layer respectively.
m_1	Mass of impactor (kg).
M_x, M_y, M_{xy}	Resultant Moments per unit length (N. m / m) respectively.
M_x^*, M_y^*, M_{xy}^*	High-order stress-resultants (N m).
M_x, M_y, M_{xy}	Resultant Moments per unit length (N. m / m) respectively.
M_x^*, M_y^*, M_{xy}^*	High-order stress-resultants (N m).
N_x,N_y,N_{xy}	Resultant forces per unit length (N/m).
P	Impact load (N).
p_o	Maximum impact force during impact duration (N).
Q_{ij}	Element of elasticity matrix (N/m^2).
$\overline{Q}_{ij}$	Transformed stress-strain relation (N/m^2).
Q_x, Q_y	Shear forces per unit length (N/m).
Q_x^*, Q_y^*	High-order shear forces (N. m).
R_1	Radius of a spherical impactor (m).
S, F, C	Simply supported, free, and clamped edge respectively.
T	Time (s).
u, v, w	Displacement in the x, y and z directions (m) respectively.
V_1 , V_2	Initial velocity of impactor and target (m/sec) respectively.
ϕ_x, ϕ_y	Rotations of the transverse normal in xz and yz plane.
υ_{ij}	Poisson's ratio giving the strain in j direction caused by a strain in i direction.
ε	Normal strain.
θ	Angle of layer lamination (degree).
σ	Normal stress (N / m^2).
τ	Shearing stress (N / m^2).
μ	Local indentation (m).
μ_1	Maximum deformation (m).
θ_i	Higher-order transverse cross section deformation modes.